

Supporting Information

The Balance of Structural Compatibility and Distortion in Titanium Source for the Preparation of High Performance $\text{Na}_2\text{Ti}_6\text{O}_{13}$ Anode

Qian Li, Changyan Hu, Yihua Liu, Ruoyang Wang, Feng Chen, Tingru Chen, Zhenguo Wu*,
Xiaodong Guo

*School of Chemical Engineering, Sichuan University
Chengdu 610065, P. R. China.*

*Corresponding author.

E-mail address: Zhengguowu@scu.edu.cn

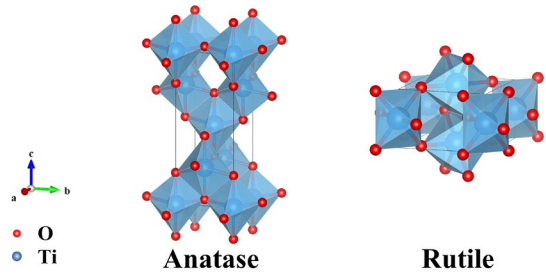


Fig. S1. Crystal structures of two TiO_2 polymorphs based on their unit cells.

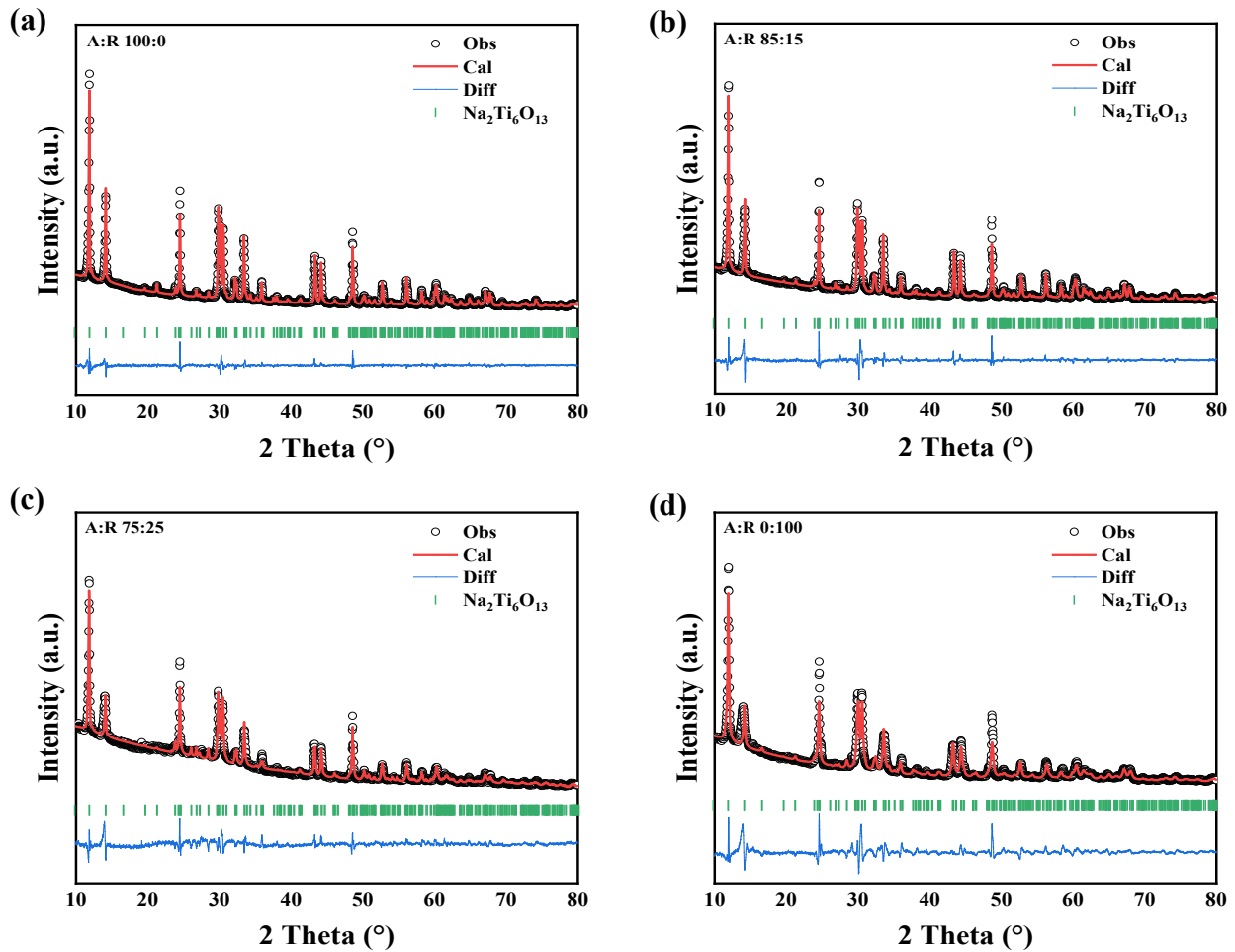


Fig. S2. Rietveld detailed map and laboratory XRD data of materials synthesized from different crystalline TiO₂ (a) A: R 100:0; (b) A: R 85:15; (c) A: R 75:25; (d) A: R 0:100. The black lines correspond to the observed data; the red lines indicate the calculated profiles, and the blue lines are the difference between the observed and calculated profiles. The green marks indicate the bragg reflection of Na₂Ti₆O₁₃.

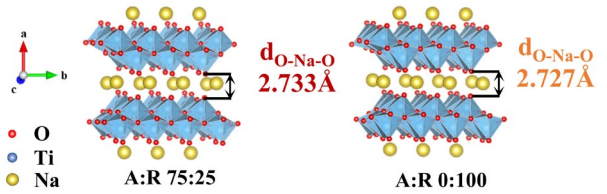


Fig. S3. Schematic crystal structure of $\text{Na}_2\text{Ti}_6\text{O}_{13}$: A: R 75:25 (left), A: R 0:100 (right).

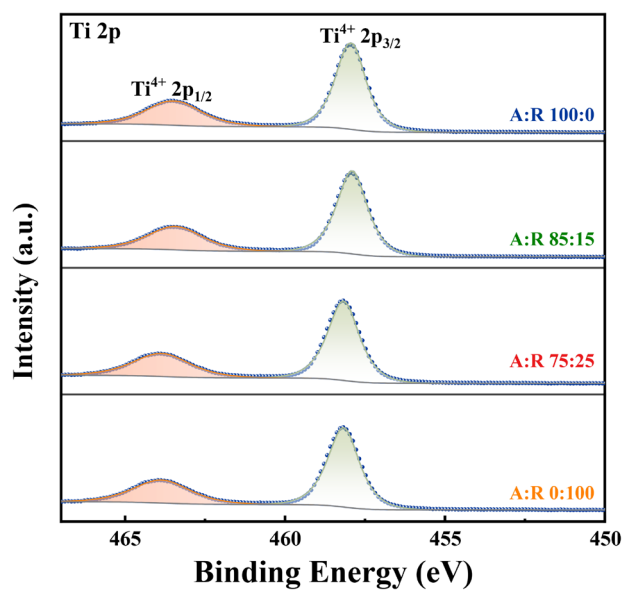


Fig. S4. XPS spectra of $\text{Na}_2\text{Ti}_6\text{O}_{13}$ compound $\text{Ti } 2\text{p}$ prepared from different titanium sources.

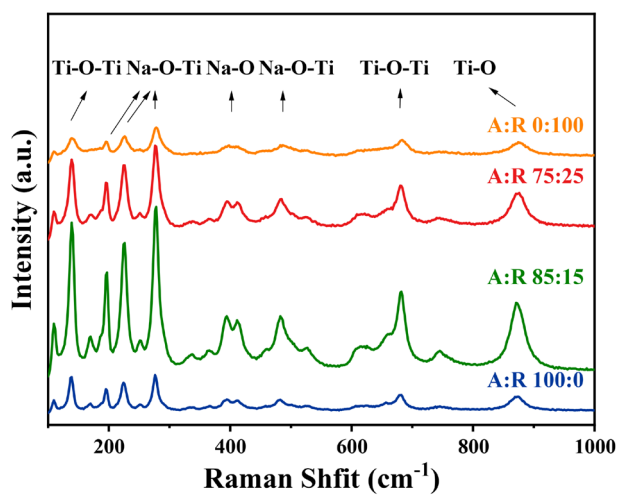


Fig. S5. Raman spectra of $\text{Na}_2\text{Ti}_6\text{O}_{13}$ (a) A: R-100:0, (b) A: R-85:15, (c) A: R-75:25, (d) A: R-0:100.

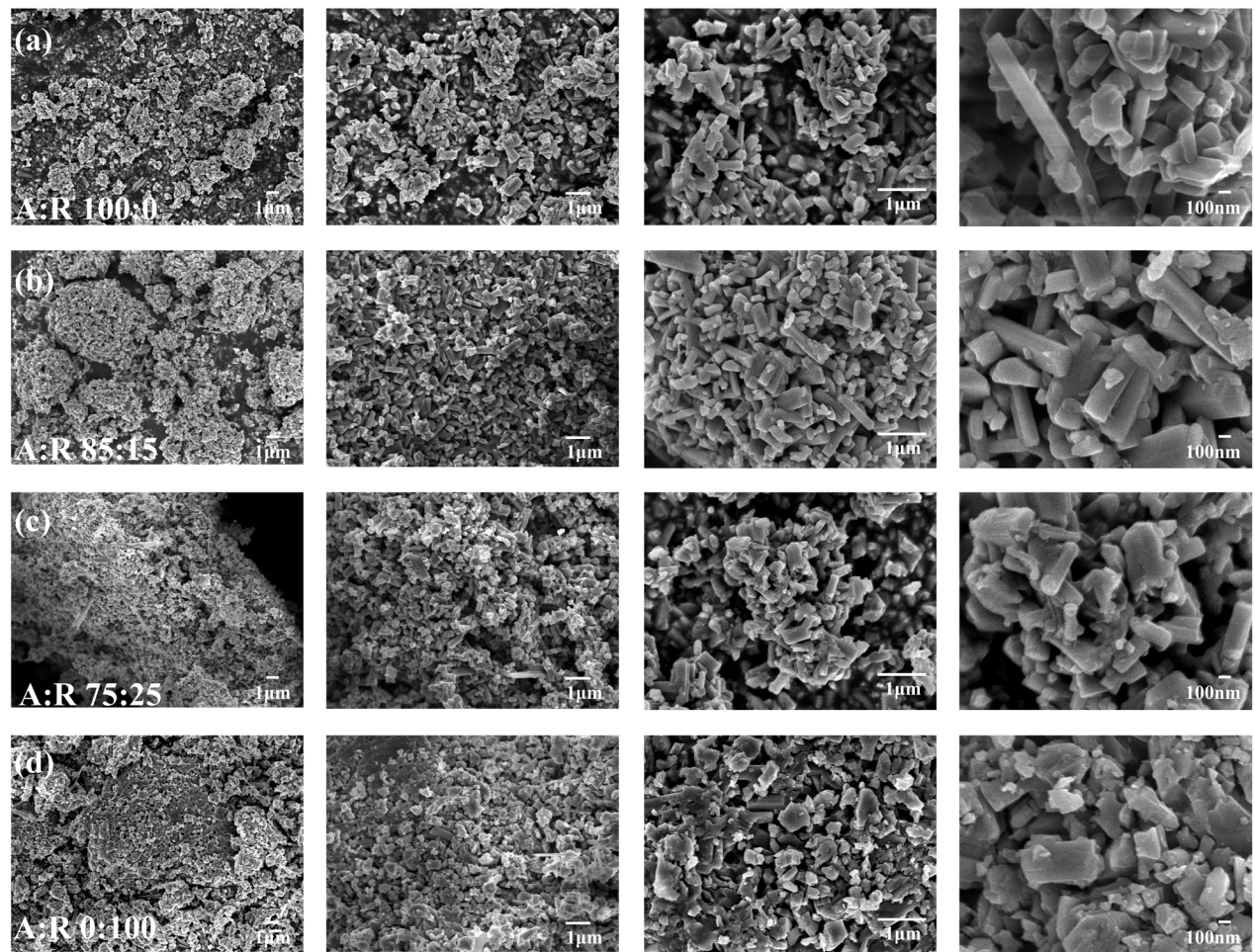


Fig. S6. SEM micrographs of NTO materials synthesized from different raw materials (a) A: R-100:0, (b) A: R-85:15, (c) A: R-75:25, (d) A: R-0:100.

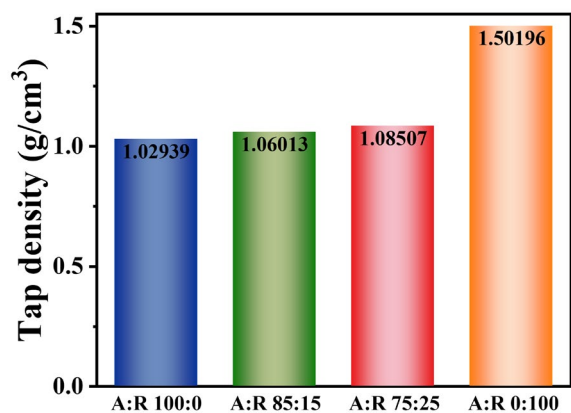


Fig. S7. Tapped density of NTO materials synthesized from different raw materials.

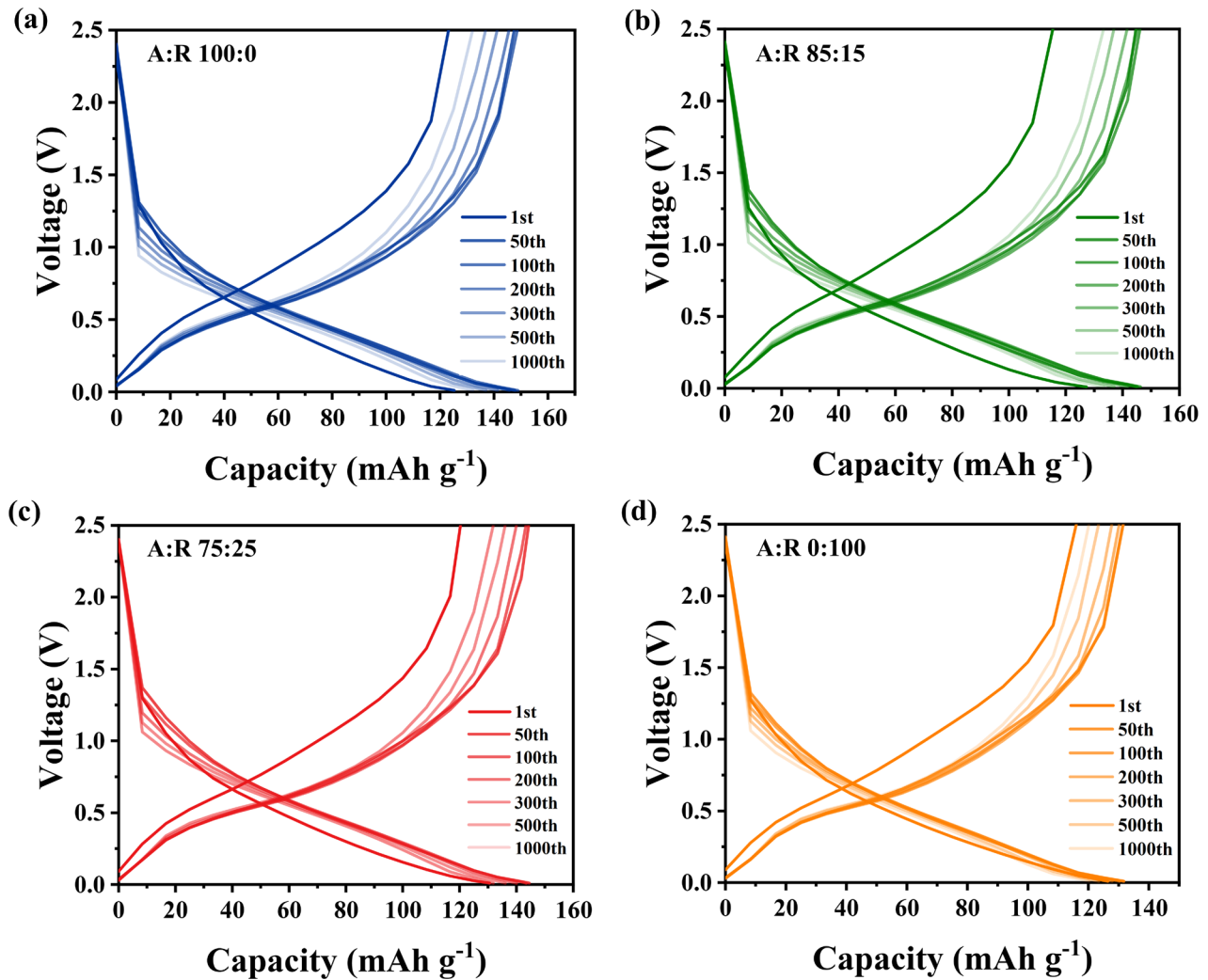


Fig. S8. Discharge-charge curves of (a) A: R-100:0, (b) A: R-85:15, (c) A: R-75:25, (d) A: R-0:100 at 1000 mA g⁻¹.

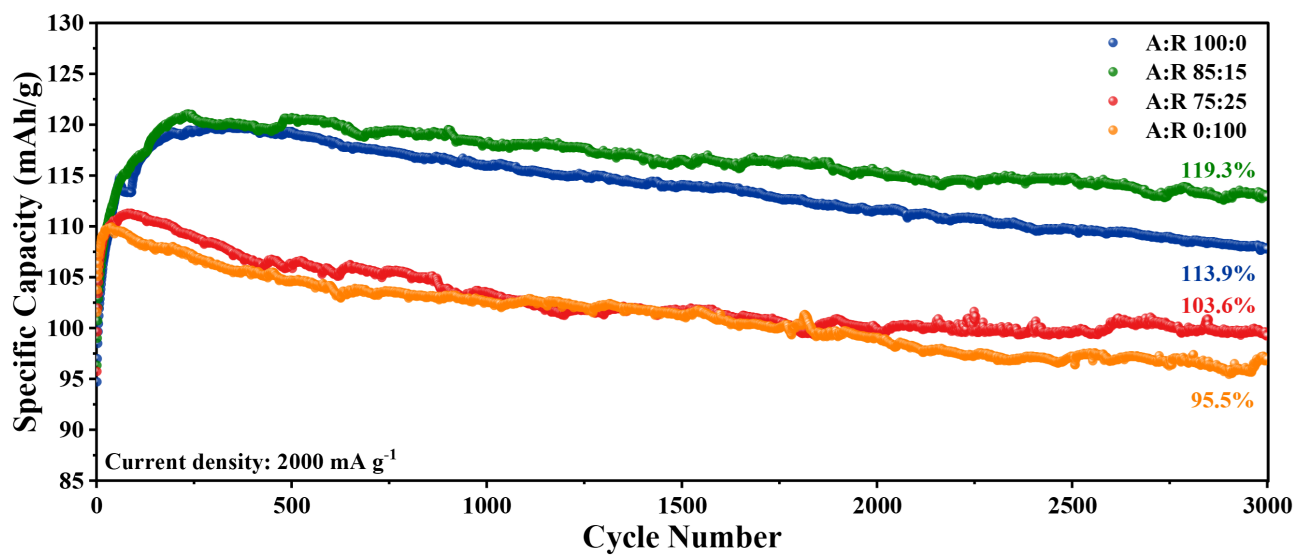


Fig. S9. The cycling performance of NTO at 2000 mA g^{-1} .

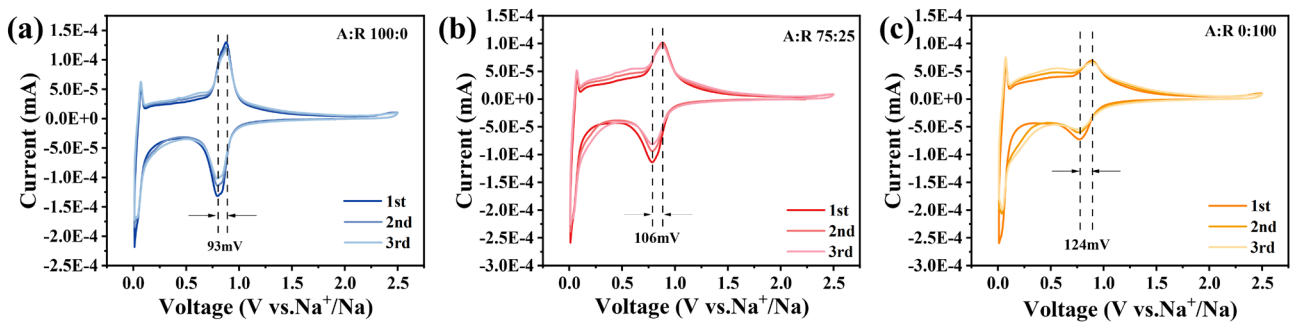


Fig. S10. The first three CV curves of NTO materials synthesized from different titanium sources (a) A: R-100:0, (b) A: R-85:15, (c) A: R-0:100 at 0.1 mv^{-1} at 30°C .

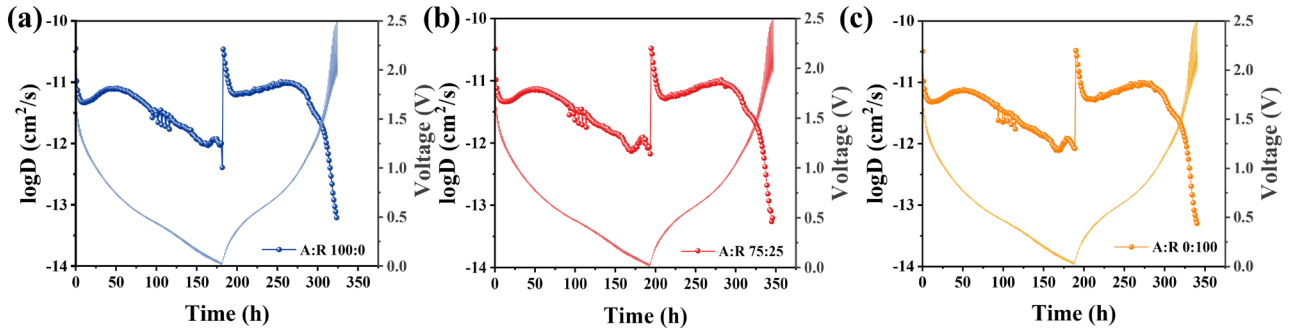


Fig. S11. GITT curves of NTO prepared from different raw materials at 30°C and corresponding Na^+ diffusion coefficients (D_{Na^+}).

The diffusion coefficient was calculated using the following equation:

$$D_{\text{Na}^+} = \frac{4}{\pi\tau} \left(\frac{m_B V_m}{M_B S} \right)^2 \left(\frac{\Delta E_s}{\Delta E_\tau} \right)^2 \quad (1)$$

D_{Na^+} represents the Na^+ diffusion coefficient at the negative electrode. τ (s) denotes the duration of the applied current during the galvanostatic intermittent titration process. V_m ($\text{cm}^3 \text{ mol}^{-1}$) is the molar volume of the active material at the negative electrode, while m_B (g) and M_B (g mol^{-1}) correspond to the mass and molar mass of the active material, respectively. S (cm^2) signifies the surface area of the electrode. ΔE_s and ΔE_τ represent the voltage change during the charging/discharging process and the voltage shift from the resting state to the equilibrium state, respectively.

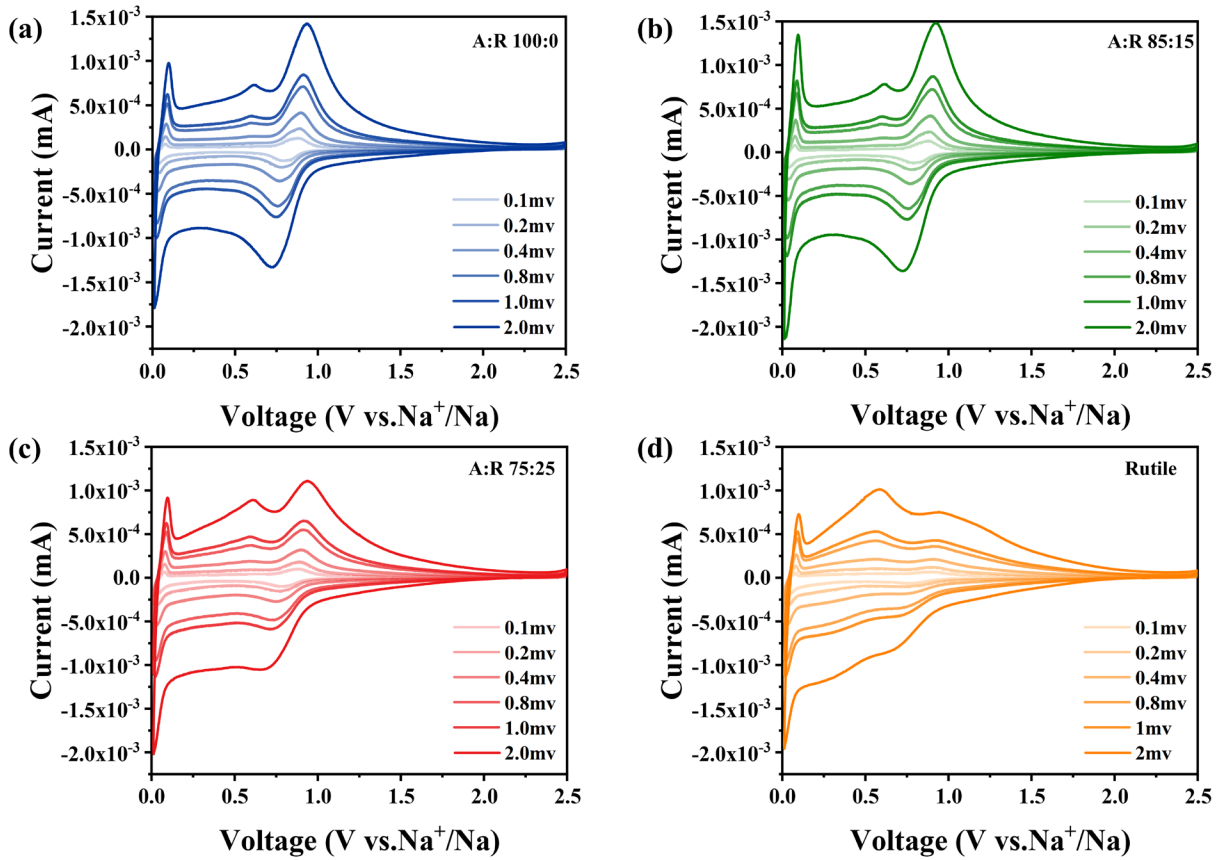


Fig. S12. CV curves of different titanium NTO composite at different scan rates (a) A: R-100:0; (b) A: R-85:15; (c) A: R-75:25 and (d) A: R-0:100 at 30°C.

The value of b is calculated from the relationship between the response current (i) and the scan rate (v) at a certain potential:

$$i_{(v)} = av^b \quad (2)$$

$$\log i_v = b \log v + \log a \quad (3)$$

The ratio of the two components is quantified according to the equation following:

$$i_{(v)} = k_{1(v)}v + k_{2(v)}v^{1/2} \quad (4)$$

$$i_{(v)}/v^{1/2} = k_{1(v)}v^{1/2} + k_{2(v)} \quad (5)$$

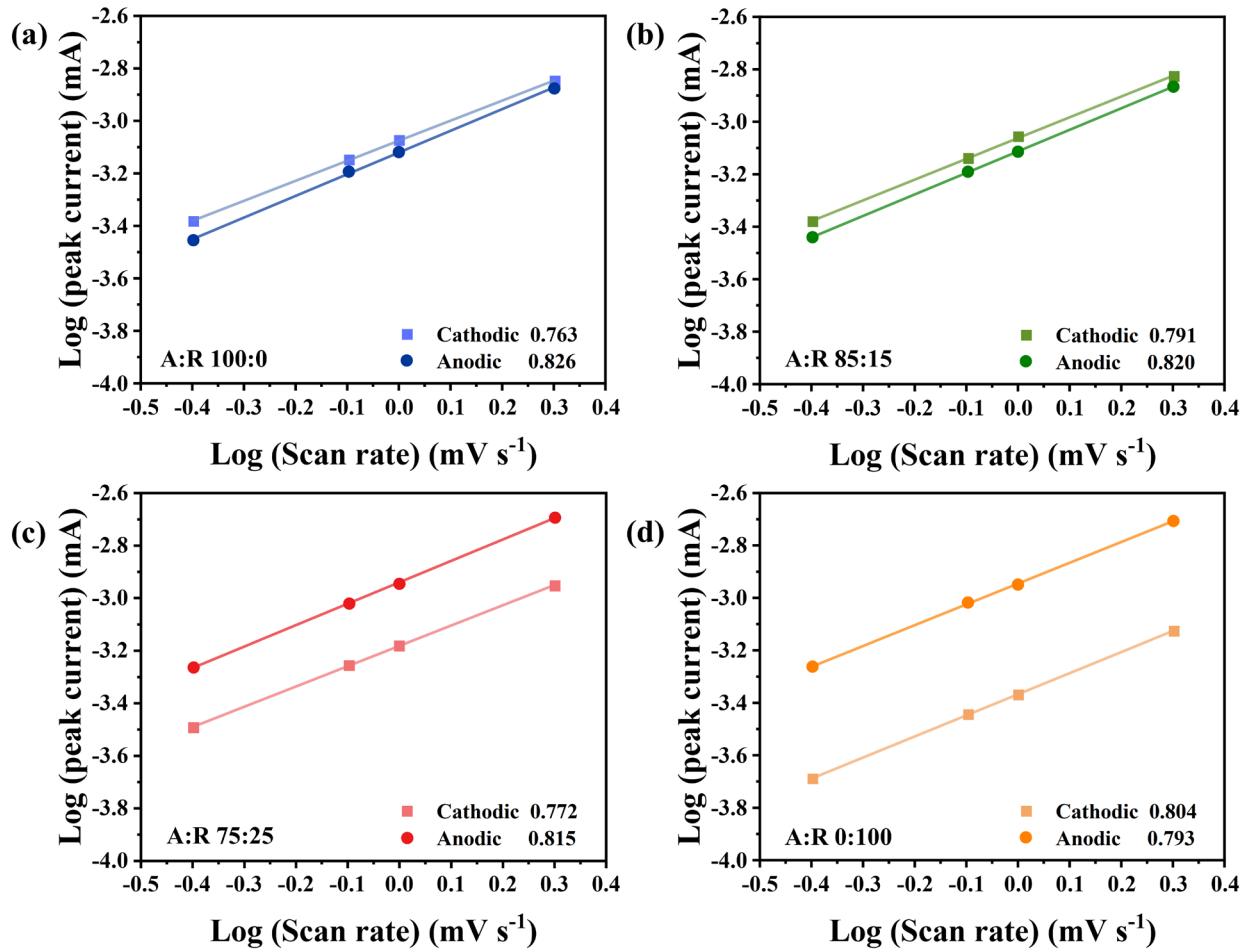


Fig. S13. The plot of the peak current (i) as a function of the square root of scanning rates ($v^{1/2}$)

is calculated from CV curves in Figure S12 (a) A: R-100:0; (b) A: R-85:15; (c) A: R-75:25 and (d) A: R-0:100 at 30°C.

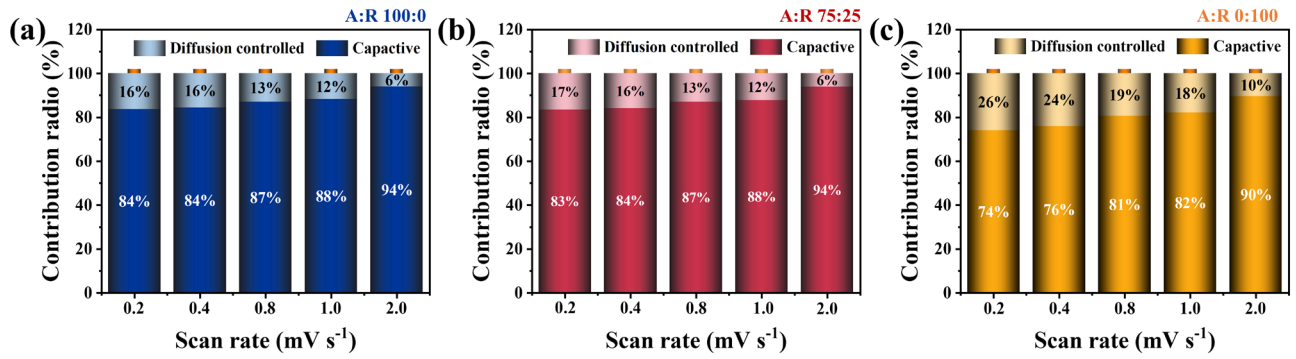


Fig. S14. The ratio of capacitance/diffusion ratio control contribution of NTO materials synthesized from different titanium sources (a) A: R-100:0; (b) A: R-75:25; (c) A: R-0:100 at 0.1 mv^{-1} at 30°C .

Table S1. Crystallographic Data of Two TiO₂ Polymorphs: Rutile-TiO₂, Anatase-TiO₂.

Polymer	Space group	a [Å]	b [Å]	c [Å]	Ti–O bond lengths [Å]	Ti–Ti interatomic distance [Å] ^a
Rutile	P42/mnm (No.136)	4.594	4.594	2.959	1.99×2 1.95×4	2.96×2 (ES) 3.57×8 (VS)
Anatase	I41/amd (No. 141)	3.784	3.784	9.515	1.98×2 1.93×4	3.04×4 (ES) 3.04×4 (ES)

^aES and VS denote edge and vertex sharing in the connection of the TiO₆ octahedra, respectively.

Table S2. Rietveld refinement parameters of Na₂Ti₆O₁₃.

	a [Å]	b [Å]	c [Å]	V [Å]	β [°]	R _{wp} (%)
A: R-100:0	15.111	3.745	9.170	512.512	99.055	5.57
A: R-85:15	15.117	3.745	9.165	512.352	99.125	8.45
A: R-75:25	15.132	3.744	9.151	511.743	99.228	9.84
A: R-0:100	15.156	3.739	9.156	511.570	99.585	10.10

Table S3. Summary Table of Detailed BET Parameters.

	BET specific Surface area (m ² g ⁻¹)	Pore volume (cm ³ g ⁻¹)	Average Pore size (nm)
A: R-100:0	4.886	0.02539	2.078
A: R-85:15	4.058	0.02355	2.321
A: R-75:25	2.138	0.01095	2.050
A: R-0:100	0.767	0.00877	4.576

Table S4. Calculated sodium ion diffusion coefficients for NTO of different titanium raw materials.

Sodium ion diffusion (cm ² s ⁻¹)	
A: R-100:0	6.16*10 ⁻¹⁴ -3.54*10 ⁻¹¹
A: R-85:15	1.05*10 ⁻¹³ -3.55*10 ⁻¹¹
A: R-75:25	5.50*10 ⁻¹⁴ -3.31*10 ⁻¹¹
A: R-0:100	5.03*10 ⁻¹⁴ -3.29*10 ⁻¹¹